





## Corrosion of Zn-Ni coated reinforcing steel in simulated concrete pore solutions


Mihael M. Bučko<sup>a</sup>, Ljubica M. Radović<sup>b</sup>, Marko N. Dimitrijević<sup>c</sup>, Radovan M. Karkalić<sup>d</sup>, Jelena B. Bajat<sup>e</sup>


<sup>a</sup> University of Defence in Belgrade, Military Academy, Department for Military Chemical Engineering, Belgrade, Republic of Serbia, e-mail: mihael.bucko@va.mod.gov.rs, **corresponding author**, ORCID ID:  <https://orcid.org/0000-0001-6992-8841>

<sup>b</sup> Military Technical Institute, Belgrade, Republic of Serbia, e-mail: ljubica.radovic@mod.gov.rs, ORCID ID:  <https://orcid.org/0000-0002-5204-983X>

<sup>c</sup> University of Defence in Belgrade, Military Academy, Department for Military Chemical Engineering, Belgrade, Republic of Serbia, e-mail: markodimitrijevic2402@gmail.com, ORCID ID:  <https://orcid.org/0009-0009-2517-6532>

<sup>d</sup> University of Defence in Belgrade, Military Academy, Department for Military Chemical Engineering, Belgrade, Republic of Serbia, e-mail: rkarkalic@yahoo.com, ORCID ID:  <https://orcid.org/0000-0002-8074-7264>

<sup>e</sup> University of Belgrade, Faculty of Technology and Metallurgy, Belgrade Republic of Serbia, e-mail: jela@tmf.bg.ac.rs, ORCID ID:  <https://orcid.org/0000-0003-0742-8176>

 <https://doi.org/10.5937/vojtehg72-54116>

FIELD: materials

ARTICLE TYPE: original scientific paper

### Abstract:

*Introduction/purpose: The anticorrosion protection of steel reinforcement bars in concrete is a critical concern in civil engineering, particularly for the construction of concrete structures intended for military applications. Currently, the most important methods for achieving this protection include the application of coatings on steel rebar (such as epoxy or hot-dip galvanized zinc), the use of stainless-steel rebar, composite rebars, or high-performance concrete that incorporates corrosion inhibitors, surface sealers, silica fume, or fly ash admixtures.*

ACKNOWLEDGMENT: This work was supported by the Ministry of Science, Technological Development and Innovation of the Republic of Serbia (Contract No. 451-03-65/2024-03/200135). The authors would also like to acknowledge support from the scientific project of the Military Academy, University of Defense in Serbia, "Research on influence of characteristics of explosive ordnance on safety in Ministry of Defense and Army of Serbia" (VA-TT/1/22-24).

*Methods: This study aims to determine whether an electroplated Zn-Ni coating of sufficient thickness can offer better long-term corrosion resistance to reinforcing steel in concrete compared to the traditional pure Zn coating typically used for this purpose. The Zn-Ni coatings produced were 40 µm thick and contained approximately 13 mass.% Ni. Scanning electron microscopy revealed a smooth and homogeneous surface morphology, although microcracks extending through the entire coating depth were observed. The protective effectiveness of the coatings was evaluated using electrochemical impedance spectroscopy, with samples immersed in various electrolytes that simulate the chemical environments present in different types of concrete.*

*Results: The measurements indicated a significantly slower dissolution rate of the corrosion product formed on the Zn-Ni coating in chloride-rich environments, compared to pure Zn.*

*Conclusion: It can be concluded that Zn-Ni alloy presents a viable alternative to pure Zn for protecting steel in concrete structures where high chloride penetration is anticipated.*

*Key words: steel rebar corrosion, Zn-Ni coating, concrete pore solution, electroplating.*

## Introduction

Corrosion of steel reinforcement in concrete structures remains a significant challenge, particularly in military applications where durability and long-term structural integrity are critical. The harsh environments to which these structures are often exposed - such as marine, coastal, or chemically aggressive conditions - accelerate corrosion processes, necessitating the development of more effective protective measures. Recent advances in corrosion prevention of steel rebar in concrete include enhancing the compactness of concrete, application of protective coatings to concrete surface, using epoxy and zinc-based coatings on steel, along with cathodic protection systems, and novel admixtures like corrosion inhibitors and nanomaterials which are mixed into concrete (Qiao et al, 2024). The steel corrosion in concrete is typically attributed to either the presence of chloride salts, which can depassivate steel in an alkaline environment, or carbonation, which lowers the alkalinity of concrete. Zinc coatings produced through the batch hot-dip galvanizing process are frequently employed as a preventative measure in reinforced concrete structures exposed to carbonation or mild chloride contamination, as Zn forms a sufficiently thick passive film (Short et al, 1996). However, the protective mechanism of Zn evolves through several stages. In fresh concrete, where  $\text{Ca}(\text{OH})_2$  is present, the slightly soluble compound

$\text{Ca}[\text{Zn}(\text{OH})_3]_2 \cdot 2\text{H}_2\text{O}$  (calcium hydroxyzincate) forms, which is primarily responsible for Zn passivation (Tan & Hansson, 2008). Studies conducted in solutions simulating carbonated concrete show that galvanized steel remains passive even after carbonation, although the reaction of calcium hydroxyzincate with  $\text{CO}_2$  leads to the formation of  $\text{CaCO}_3$  and  $\text{Zn}_5(\text{CO}_3)_2(\text{OH})_6$  (hydrozincite), which exhibits reduced protective properties (Roventi et al, 2013). Ultimately, prolonged exposure to a chloride-rich environment following concrete carbonation results in the rapid corrosion of galvanized steel, producing  $\text{Zn}_5(\text{OH})_8\text{Cl}_2 \cdot \text{H}_2\text{O}$  (zinc hydroxychloride) once the threshold concentration of chloride ions is exceeded (Roventi et al, 2014).

Nickel alloying is a widely-used technique to enhance the protective properties and hardness of zinc, and the demand for corrosion-resistant Zn–Ni coatings is substantial, primarily encompassing applications in the automotive and electronics industries (Mosavat et al, 2012). As a result, most corrosion tests on this alloy have been conducted in environments with approximately neutral solution pH. The superior corrosion resistance of Zn–Ni compared to pure Zn in neutral conditions has been attributed to several factors. One of these is the formation of complex corrosion products on the Zn–Ni alloy, which act as a barrier against the diffusion of corrosive agents. Additionally, it has been suggested that the fine cracked structure of Zn–Ni coatings distributes anodic reactions across a larger surface area, thereby reducing the likelihood of localized corrosion (Tian et al, 2009). Some researchers also propose that nickel may slow down the dehydration of  $\text{Zn}(\text{OH})_2$ , a corrosion product, into ZnO, which, in turn, delays the oxygen reduction process on the corroding surface (Wilcox & Gabe, 1993). Lastly, there is considerable evidence that the dezincification of the alloy surface results in a Ni-enriched layer, providing an improved barrier against anodic dissolution (Short et al, 1996).

Building on this background, the present study aims to investigate whether a sufficiently thick electroplated Zn–Ni coating can offer superior long-term corrosion resistance compared to pure Zn, when both are exposed to carbonation and chloride ions in an alkaline environment—conditions that closely mimic those found in concrete pores. Over the past 20 years, this possibility has been the subject of extensive research, yielding varied results depending on the experimental setup. Early studies conducted in alkaline and chloride-rich solutions concluded that Zn–Ni coatings did not demonstrate improved corrosion resistance compared to pure Zn (Short et al, 1996), though the impact of concrete carbonation was not accounted for, as the pH of the test solutions was 12.00 or higher. In contrast, more recent literature suggests that in alkaline solutions, Ni

enhances Zn passivation, reduces its dissolution rate, and as a result, Zn-Ni alloys have found widespread application in alkaline batteries (Hosseini et al, 2012; El-Sayed et al, 2015).

There is no single electrolyte that can be used in laboratory settings to universally replicate the conditions found in concrete, as many factors, such as pH levels and the concentration of corrosive agents, change over time in real concrete. However, extensive studies have been conducted to compare results obtained from concrete and simulated solutions. Based on these studies (Farina & Duffo, 2007; Moreno et al, 2004), this work employs three different electrolytes to predict and compare the behavior of Zn and Zn-Ni in three distinct environments: fresh concrete, concrete exposed to CO<sub>2</sub>, and concrete containing Cl<sup>-</sup> ions. For the corrosion testing, electrochemical impedance spectroscopy (EIS) and scanning electron microscopy (SEM) were utilized.

## Experimental section

### *Coating samples*

To compare the corrosion performance of Zn-Ni alloy-coated steel with that of galvanized steel, pure zinc was selected as a reference material for the Zn-coated steel. This choice allowed for a consistent point of comparison in all tests, eliminating the influence of various parameters that may affect the quality of the zinc coating obtained through hot-dip galvanizing.

The zinc specimens were cut from a pure Zn (99.99%) sheet with a thickness of 2 mm. The Zn-Ni alloy coatings were produced via electrochemical deposition on mild steel plates with an active surface area of 2x2 cm<sup>2</sup>, using a chloride acidic bath containing 15 g/dm<sup>3</sup> ZnO, 60 g/dm<sup>3</sup> NiCl<sub>2</sub>·6H<sub>2</sub>O, 250 g/dm<sup>3</sup> NH<sub>4</sub>Cl, and 20 g/dm<sup>3</sup> H<sub>3</sub>BO<sub>3</sub> (Bajat et al, 2001). Direct current was supplied using a PAR M173 potentiostat/galvanostat in galvanostatic mode, with a zinc plate serving as the counter electrode. Prior to the deposition of the Zn-Ni alloy, the steel substrate underwent several preparatory treatments: abrasion with emery papers of grades 600, 1000, and 1200, degreasing in a saturated NaOH solution in ethanol, pickling with 2 mol/dm<sup>3</sup> HCl for 30 seconds, and finally rinsing with distilled water.

The plating process was conducted at 40 °C without stirring, with deposition times adjusted to achieve coating thicknesses of up to 40 μm, as verified by a DUALSCOPE MPOR coating thickness measuring instrument.

### Characterization techniques

The morphology and composition of the freshly prepared Zn-Ni coatings were analyzed using a scanning electron microscope (SEM), a Tescan VEGA TS 5130 MM, equipped with an energy-dispersive spectroscopy (EDS) system (INCAPenta-FETex3, Oxford Instruments). For the SEM images of the cross-section, the samples were embedded in epoxy resin, then cut and mechanically polished using various grades of emery paper.

To compare the corrosion behavior of the samples, pure Zn and Zn-Ni alloy-coated steel were sequentially exposed to three different solutions that simulated fresh, carbonated, and chloride-rich concrete environments, as described in (Farina & Duffo, 2007; Moreno et al, 2004), i.e., the same samples were exposed over a total period of 21 days, divided into three cycles of 7 days each. The solutions were prepared using analytical grade reagents and double-distilled water, with their compositions outlined in Table 1.

Table 1 – Composition of the simulated concrete pore solutions

Composition	Exposure time	Corrosion media simulating
Saturated $\text{Ca}(\text{OH})_2$	7 days	Fresh concrete
$0.015 \text{ mol dm}^{-3} \text{ NaHCO}_3 + 0.005 \text{ mol dm}^{-3} \text{ Na}_2\text{CO}_3$ , pH 9.50	7 days	Carbonated concrete
$0.015 \text{ mol dm}^{-3} \text{ NaHCO}_3 + 0.005 \text{ mol dm}^{-3} \text{ Na}_2\text{CO}_3 + 0.5 \text{ mol dm}^{-3} \text{ NaCl}$	7 days	Carbonated concrete with chloride penetration

The corrosion processes in the solutions outlined in Table 1 were monitored using electrochemical impedance spectroscopy (EIS). All measurements were conducted at room temperature in a Pyrex glass three-electrode cell, which included a platinum mesh counter electrode and a saturated calomel reference electrode, with electrode potential measured through a Luggin capillary. The EIS studies involved applying a sinusoidal voltage of 10 mV amplitude at the open circuit potential of the working electrode, utilizing a ZRA Reference 600 potentiostat from Gamry Instruments. The frequency ranged from 100 kHz to 10 mHz. The working electrode consisted of a coated sample placed in a Teflon holder, with an exposed area of 1 cm<sup>2</sup>. Data fitting for the impedance was performed using Gamry Instruments Echem Analyst software. The impedance spectrum was recorded at 24-hour intervals over a total immersion period of 21 days.

## Results and discussion

### *The electrodeposition of Zn-Ni coating of a sufficient thickness*

The first part of the results focuses on two key requirements for producing a coating capable of withstanding the conditions in concrete: the optimal chemical composition and a sufficient thickness of the electroplated Zn–Ni coating. The Zn–Ni coatings were electrodeposited using a constant current density of 20 mA/cm<sup>2</sup>, a parameter based on our previous research (Bajat & Mišković-Stanković, 2004), to ensure the production of non-dendritic deposits with a nickel content of 12–15 wt.%. SEM images (both normal and cross-sectional views) of Zn–Ni coatings with two different thicknesses are shown in Figure 1, along with their elemental compositions. The images reveal that the surface morphology was smooth and uniform for both specimens, characterized by hemispherical clusters. In the thinner sample, a fine-grained, smoother morphology was observed, with clusters less than 1 µm in size (Figure 1a). In contrast, the thicker coating exhibited larger clusters, approximately 10 µm in size, with a more pronounced cauliflower-like morphology (Figure 1b). This type of surface appearance has been previously reported for Zn–Ni electrodeposits containing a single γ–Zn–Ni phase (Mosavat et al, 2012).

The cross-sectional SEM analysis confirms that the coatings exhibit uniform thickness and homogeneity throughout their depth (Figures 1c, d). However, both samples contained through-thickness microcracks. Defects such as cracks and through-thickness pores are common in electroplated Zn–Ni coatings with a nickel content exceeding 8–10 wt.% (Kwon et al, 2016). These cracks are attributed to the inherent lattice strain associated with the formation of the γ–Zn–Ni phase, making it challenging to achieve a continuous coating layer (Kwon et al, 2016, Sriraman et al, 2013). Despite this, studies have shown that cracked Zn–Ni coatings still offer superior sacrificial corrosion protection compared to Zn and Cd coatings, particularly in NaCl environments (Sriraman et al, 2013). Therefore, in this work, the corrosion performance of 40 µm thick Zn–Ni alloy coatings was further compared with that of pure Zn coatings. The semiquantitative EDS analysis (Figure 1e) confirms that the Zn–Ni coatings contain an average of ~13 wt.% Ni throughout their depth.

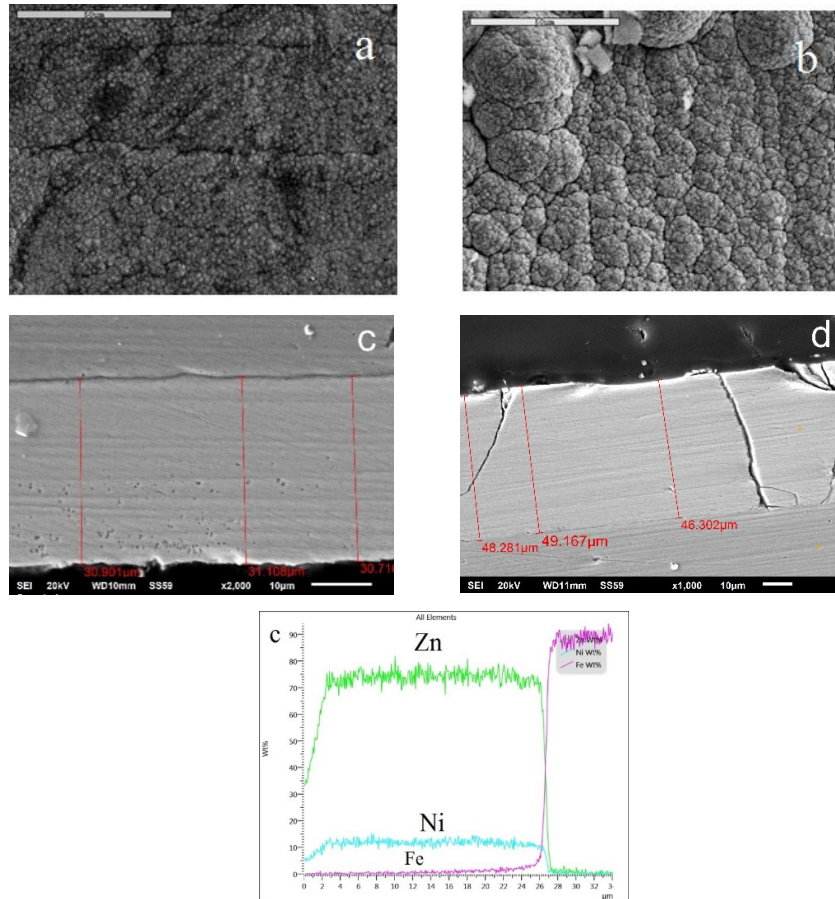


Figure 1 – SEM/EDS analysis of Zn–Ni coatings: a) b) surface morphology (scale bar length is 50 μm), (c, d) cross section, e) EDS line analysis through a coating cross section. Coating thickness of 30 μm (a, c) and 40 μm (b, d)

The hot-dip galvanizing process, a standard method for coating reinforcing steel, typically results in a Zn–Ni alloy containing a maximum of 0.5 wt.% Ni, as higher nickel levels have been associated with disadvantages such as a rough surface and insufficient coating thickness (Emel’yanov et al, 2009). However, much of the literature on the corrosion resistance of Zn–Ni alloy coatings in neutral and alkaline media suggests that the best performance is achieved with a nickel content in the range of 11–15 wt.%, where the coating consists predominantly of the  $\gamma$ -Zn<sub>21</sub>Ni<sub>5</sub> phase (Mosavat et al, 2012; Short et al, 1996; Bajat et al, 2001).

Electrodeposition has been found to successfully achieve this optimal composition, which is why it was selected as the coating method for reinforcing steel in this study.

Most scientific studies on Zn–Ni electrodeposition have focused on achieving a maximum coating thickness of around 30 μm. Furthermore, standard specifications for atmospheric corrosion protection of steel typically require Zn–Ni electroplated coatings to be only 10 μm thick (ASTM, 2019). In contrast, ASTM A767, the Standard Specification for Zinc-Coated (Galvanized) Steel Bars for Concrete Reinforcement, mandates a minimum zinc coating thickness of 85 μm (equivalent to 6.1 g/m<sup>2</sup> by mass) for concrete applications. Therefore, this study aimed to investigate whether it is possible to produce an adherent and homogeneous Zn–Ni coating of greater thickness (>30 μm) through electrodeposition, comparable to the commercial zinc layers used in concrete reinforcement. Notably, "thick" Zn–Ni electrodeposits have been reported in the past, with thicknesses of 40 μm (Ravindran & Muralidharan, 2006) and 100 μm (El-Sayed et al, 2015). In both cases, smooth, semi-bright, and homogeneous coatings were achieved by using additives such as sodium lauryl sulfate (El-Sayed et al, 2015) or substituted aldehydes (Ravindran & Muralidharan, 2006).

***Electrochemical impedance spectroscopy results***

The EIS studies were conducted on a daily basis for both the Zn bulk plate and the Zn–Ni coated samples, with each being successively exposed to three different corrosion media simulating fresh concrete, carbonated concrete, and carbonated concrete containing chloride salts. The EIS Nyquist spectra for the Zn plate and the Zn–Ni coated samples, recorded in these three different solutions, are presented in Figures 2, 3, and 4, respectively.

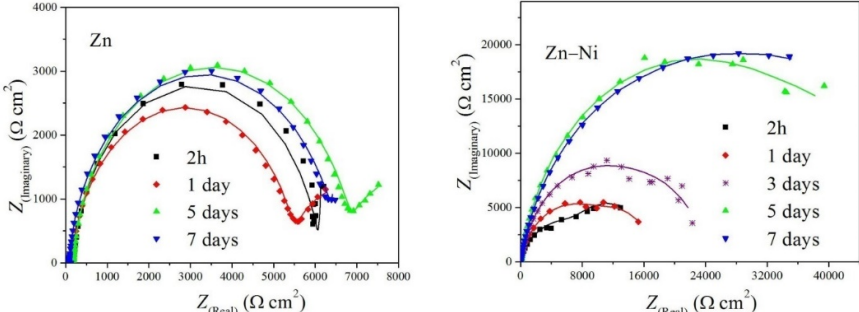


Figure 2 – Nyquist plots for the Zn plate and the Zn–Ni coated reinforcing steel in saturated Ca(OH)<sub>2</sub> during the first 7-day cycle of immersion



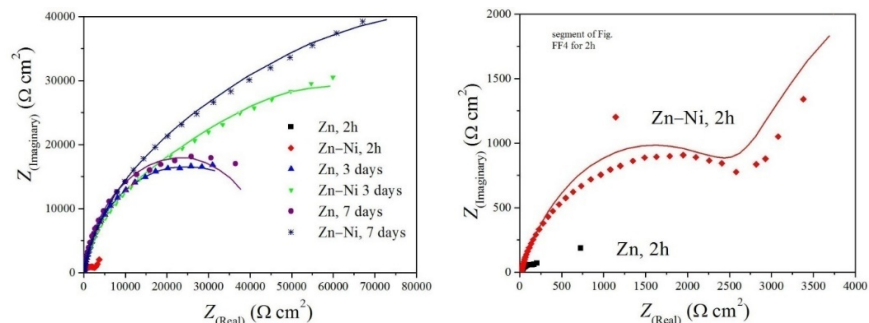


Figure 3 – Nyquist plots for the Zn plate and the Zn–Ni coated reinforcing steel in  $0.015 \text{ mol dm}^{-3} \text{ NaHCO}_3 + 0.005 \text{ mol dm}^{-3} \text{ Na}_2\text{CO}_3$  during the second 7-day cycle of immersion

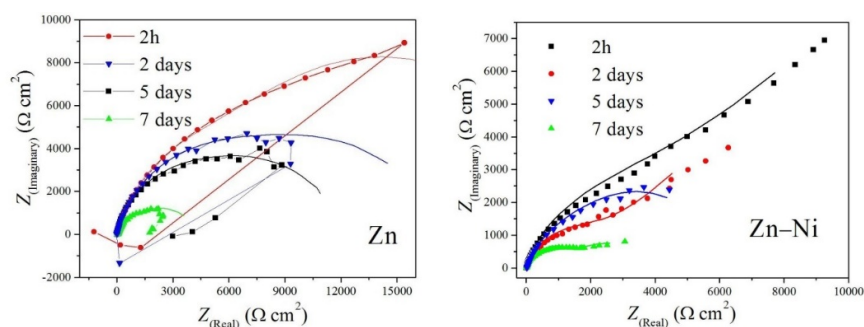


Figure 4 – Nyquist plots for the Zn plate and the Zn–Ni coated reinforcing steel in  $0.015 \text{ mol dm}^{-3} \text{ NaHCO}_3 + 0.005 \text{ mol dm}^{-3} \text{ Na}_2\text{CO}_3 + 0.5 \text{ mol dm}^{-3} \text{ NaCl}$  during the 3<sup>rd</sup> 7-day cycle of immersion. For Zn, the recorded data are presented as dot+line, so that the inductive behaviour is clearly visible

Throughout the 21-day immersion in the three different solutions, the EIS response for all the samples exhibited two distinct patterns: either a depressed semicircular arc followed by a second arc or an ill-defined tail, or a single depressed arc resulting from the superposition of two semicircles. Based on equivalent circuit (EC) studies for corrosion processes of metal coatings covered by protective corrosion products (Hamlaoui et al, 2008), this system can be modeled using the equivalent circuit shown in Figure 5. This circuit effectively accounts for the two time constants observed in the impedance plots, whether they are well-separated or merged. The first time constant, observed at high frequencies, corresponds to the properties of the corrosion product layer,

while the second time constant at low frequencies characterizes the corrosion process occurring at the interface between the corrosion product and the metal.

In this model,  $R_s$  represents the electrolyte resistance between the sample and the Luggin capillary. The  $R_1/Q_1$  pair represents the electrolytic resistance and capacitance within defects of the corrosion product layer, while the  $R_2/Q_2$  pair refers to the charge transfer resistance and the double-layer capacitance associated with the metal corrosion process in the cavities of the protective layer (Hamlaoui et al, 2008). To account for the non-ideal capacitive behavior at the interface between the sample and the solution, which is responsible for the appearance of depressed Nyquist semicircles, a constant phase element (CPE) was applied to replace pure capacitance for fitting the spectra (Hsu & Mansfeld, 2001).

The model shown in Figure 5 assumes that the corrosion product film does not completely cover the metal and should be considered a defective layer rather than a homogeneous one. The fitting results of the experimental data using this EC model are represented by the solid lines in Figures 2, 3, and 4, which show a good agreement with the experimental data. The calculated resistance parameters for the simulated diagrams are presented in Table 2. Additionally, the overall corrosion resistance of the samples was evaluated by calculating the total polarization resistance as the sum of  $R_1$  and  $R_2$  (Cao et al, 2017; Wu et al, 2017), with the calculated values depicted in Figure 6.

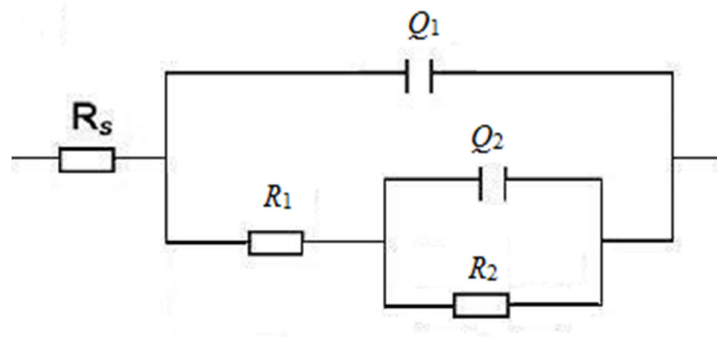


Figure 5 – Equivalent electrical circuit of the corroding Zn–Ni coated steel or the pure Zn plate in different electrolytes simulating concrete media

Table 2 – The values of the resistance parameters  $R_1$  and  $R_2$  for different corroding samples in three different media

Immersion period	Pure Zn sample		Zn–Ni coating, 40 $\mu\text{m}$ thick	
Saturated $\text{Ca}(\text{OH})_2$	$R_1 / \text{k}\Omega \text{ cm}^2$	$R_2 / \text{k}\Omega \text{ cm}^2$	$R_1 / \text{k}\Omega \text{ cm}^2$	$R_2 / \text{k}\Omega \text{ cm}^2$
2h	5.201	1.037	10.16	7.416
1 day	5.409	2.447	12.72	4.557
3 days	-	-	19.80	3.933
5 days	6.770	2.332	43.74	8.511
7 days	6.413	2.667	40.47	19.26
<b>0.015 mol <math>\text{dm}^{-3}</math> <math>\text{NaHCO}_3</math> + 0.005 mol <math>\text{dm}^{-3}</math> <math>\text{Na}_2\text{CO}_3</math></b>				
2h	0.21	0.009	3.322	5.441
3 days	32.78	12.19	32.28	79.49
7 days	39.38	5.757	37.26	131.8
<b>0.015 mol <math>\text{dm}^{-3}</math> <math>\text{NaHCO}_3</math> + 0.005 mol <math>\text{dm}^{-3}</math> <math>\text{Na}_2\text{CO}_3</math> + 0.5 mol <math>\text{dm}^{-3}</math> <math>\text{NaCl}</math></b>				
2h	12.07	12.53	4.10	16.57
2 days	9.628	7.745	5.17	5.986
5 days	7.111	4.802	4.003	3.654
7 days	2.355	1.974	2.213	1.010

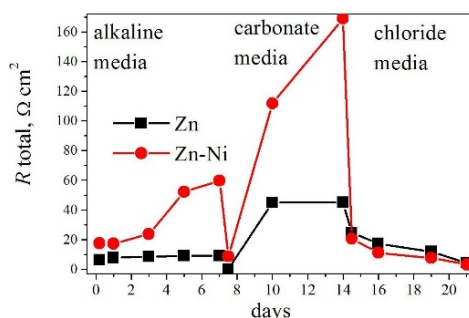


Figure 6 – The change of the total resistance with immersion time, for the pure Zn plate and the Zn–Ni corroding samples

The fitted resistance values for both the Zn plate and the Zn–Ni coated steel during the first seven days of testing exhibit high values, in the order of several  $\text{k}\Omega \text{ cm}^2$ , which progressively increase over time. These elevated  $R$  values indicate the formation of a protective film on both the pure Zn and the Zn–Ni alloy surfaces in saturated  $\text{Ca}(\text{OH})_2$ . This observation aligns

with the findings of Farina & Duffo (2007) who demonstrated that a stable passive film can form on zinc in a fresh concrete environment within just 40 minutes. Similarly, earlier studies have confirmed the formation of a passive layer on Zn–Ni alloys in alkaline corrosion media (El-Sayed et al, 2011). For pure Zn, the relatively stable resistance values suggest that the characteristics of the passive layer remain largely unchanged throughout the seven-day testing period. In contrast, the Zn–Ni coating shows a marked increase in the diameter of the impedance semicircles over time, indicating that the porosity of the protective layer decreases and its thickness increases with prolonged exposure to  $\text{Ca}(\text{OH})_2$ . The results obtained from our measurements may be compared with those reported by Wang et al. (2019), where the corrosion behavior of Zn–Al, Zn–Mg, and Zn–Mg–Al coatings was monitored in an alkaline electrolyte designed to simulate concrete pore conditions. In their study, after a 7-day immersion period, the most favorable corrosion performance was observed for the Zn–0.5Mg and Zn–0.5Mg–0.2Al alloys which exhibited a corrosion current density of approximately  $50 \mu\text{A cm}^{-2}$ , correlating to a polarization resistance of around  $500 \Omega \text{ cm}^2$ . This comparison highlights that the Zn–Ni coating employed in our investigation provides superior protective characteristics in alkaline solutions.

Following the initial 7-day exposure in an alkaline medium, the samples were transferred to a carbonate-rich electrolyte without any cleaning procedures, ensuring that the corrosion products formed in the alkaline environment remained on the surface. This step aimed to investigate how concrete carbonation influences the modification of the protective layer on Zn and Zn–Ni alloy coatings, previously formed in a solution simulating fresh concrete. Figure 3 illustrates the Nyquist plot of both Zn and Zn–Ni coatings, revealing a similar corrosion behavior in carbonated media. The spectra recorded 2 hours after the immersion show very low initial impedance values, likely due to rapid chemical changes in the passive film formed earlier in the alkaline solution. This behavior persists for up to 8 hours. However, after 8 hours, the corrosion resistance of both coatings increases progressively with time, reaching a total impedance of  $140 \text{ k}\Omega$  for Zn–Ni and  $70 \text{ k}\Omega$  for Zn after 7 days. The shape of the impedance curves corroborates previous findings on Zn corrosion in carbonated media where independent studies have demonstrated rapid metal passivation. Nevertheless, the composition of the passive layer varies depending on experimental conditions such as temperature, carbonate/bicarbonate content, and pH, ranging from a thin ZnO film (Kaesche, 1964) to hydrozincite which is specific to concrete pores (Roventi et al, 2013).

Following the second exposure cycle, the experiment proceeded into the final 7-day cycle where the samples were immersed in a solution simulating chloride penetration into carbonated concrete. It is important to note that, similarly to the second cycle, the impedance response was not from the bare metal, but from the metal coated with the corrosion products formed in the alkaline phase and later modified in the carbonate electrolyte. The visual appearance of the two specimens differed at the start of immersion in the chloride solution: the Zn surface appeared white and smooth, while the Zn–Ni surface was flat and black. Over the 7-day exposure period to the chloride-rich electrolyte, Zn–Ni retained its black appearance, while the white product on Zn continued to grow in volume and began peeling off the sample. It is likely that the white product was zinc hydroxychloride, as it is known to occupy approximately 3.6 times the volume of the original zinc (Sistonen et al, 2008).

Figure 4 presents the Nyquist plots recorded for the samples exposed to the simultaneous action of carbonation and chloride ions (i.e., the 3<sup>rd</sup> immersion cycle) at four different immersion times. As immersion time increases, the total impedance decreases in both diagrams, indicating the degradation of the corrosion product layer on the coatings. Chloride ions, known as strong anodic activators, create pores in the corrosion product layer, allowing them to penetrate through and attack the underlying metal (Padilla & Alfantazi, 2014). The Nyquist diagrams in Figures 4a and b feature two irregularly shaped, overlapping semicircles. A key distinction between the diagrams for the Zn and Zn–Ni specimens is the presence of a low-frequency inductive loop observed throughout the immersion period in the spectra related to Zn. This low-frequency inductive behavior has been attributed to surface coverage changes by the adsorbed species involved in the Zn dissolution process and is typical when bare Zn or Zn under a poorly protective film is corroding (Padilla & Alfantazi, 2014). Unfortunately, we were unable to identify an appropriate electrical equivalent circuit to fit the low-frequency portion of the EIS spectra for Zn in Figure 4. Therefore, the resistance data were obtained by fitting only the high- and mid-frequency sections of the EIS spectra in this case.

It can be concluded from the diagrams in Figure 4 that the passive layer formed on both Zn and Zn–Ni alloy in fresh concrete does not provide adequate protection to the coatings when exposed to concrete containing  $0.5 \text{ mol dm}^{-3}$  chloride ions. However, the corrosion patterns differ significantly between Zn and Zn–Ni alloy. The voluminous corrosion product on Zn poses a significant issue, as it leads to swelling of the Zn coating, disrupts the bond between the metal and concrete, and causes concrete cracking due to product expansion (Dong et al, 2012).

Additionally, the inductive behavior observed in Figure 4 indicates that, despite its thickness, the corrosion product on Zn is discontinuous, allowing for continual corrosion of the underlying metal. These findings align with the research conducted by Roventi et al. (2014) regarding concrete exposed to  $\text{Cl}^-$  ions. In contrast, the corrosion layer formed on the Zn–Ni alloy in both fresh and carbonated concrete is thin, smooth, and black, maintaining its appearance over the 7-day exposure in chloride media. Although the protective properties of this layer diminish over time, as evidenced by the Nyquist plots, it can be asserted that significant dissolution of the Zn–Ni coating is not observed in a chloride-contaminated environment.

## Conclusion

The corrosion of steel reinforcement in concrete is very important issue in military applications, where highly durable concrete structures are often required. Hot-dip galvanization with Zn is a common method used to prevent corrosion, but it has its limitations. In this study, we propose using a thick Zn-Ni alloy coating instead, as this alloy has already proven successful as protective coating for steel bodies in the automotive industry. The Zn-Ni alloy coating with a thicknesses of 30 and 40  $\mu\text{m}$  was applied to steel through electrochemical deposition. The SEM images revealed that the coatings had a uniform, smooth surface with micro-cracks characteristic of the Zn-Ni alloy.

The main goal of this research was to compare the behavior of pure Zn and the Zn-Ni alloy in an environment simulating fresh concrete. For this purpose, three types of electrolytes were used, and the samples were sequentially exposed to each one. The first electrolyte simulated the alkaline conditions present in fresh concrete, the second simulated the penetration of  $\text{CO}_2$  into the concrete, and the third represented the entry of chloride ions into the concrete. After 21 days of testing, it was observed that in the chloride-rich electrolyte, the corrosion resistance, as measured by electrochemical impedance spectroscopy, was nearly identical for both pure Zn and the Zn-Ni alloy. However, the corrosion product on pure Zn was a bulky zinc oxide layer that tended to flake off, while on the Zn-Ni alloy, the corrosion product was a thin, smooth black layer that retained its protective properties for a longer time.

Therefore, the Zn-Ni alloy coating could be an excellent alternative for protecting steel reinforcement from corrosion in concrete structures.

## References

-ASTM. 2019. *ASTM B841-18: Standard Specification for Electrodeposited Coatings of Zinc Nickel Alloy Deposits*, 12 March. Available at: <https://doi.org/10.1520/B0841-18>.

Bajat, J.B., Maksimović, M.D., Mišković-Stanković, V.B. & Zec, S. 2001. Electrodeposition and characterization of Zn-Ni alloys as sublayers for epoxy coating deposition. *Journal of Applied Electrochemistry*, 31, pp.355-361. Available at: <https://doi.org/10.1023/A:1017580019551>.

Bajat, J.B. & Mišković-Stanković, V.B. 2004. Protective properties of epoxy coatings electrodeposited on steel electrochemically modified by Zn–Ni alloys. *Progress in Organic Coatings*, 49(3), pp.183-196. Available at: <https://doi.org/10.1016/j.porgcoat.2003.09.019>.

Cao, Z., Kong, G., Che, C. & Wang, Y. 2017. Influence of Nd addition on the corrosion behavior of Zn-5%Al alloy in 3.5 wt.% NaCl solution. *Applied Surface Science*, 426, pp.67-76. Available at: <https://doi.org/10.1016/j.apsusc.2017.07.109>.

Dong, S., Zhao, B., Lin, C., Du, R., Hu, R. & Zhang, G.X. 2012. Corrosion behavior of epoxy/zinc duplex coated rebar embedded in concrete in ocean environment. *Construction and Building Materials*, 28(1), pp.72-78. Available at: <https://doi.org/10.1016/j.conbuildmat.2011.08.026>.

El-Sayed, A.R., Abd El-Lateef, H.M. & Mohran, H.S. 2015. Effect of nickel content on the anodic dissolution and passivation of zinc–nickel alloys in alkaline solutions by potentiodynamic and potentiostatic techniques. *Bulletin of Materials Science*, 38, pp.379-391. Available at: <https://doi.org/10.1007/s12034-014-0814-7>.

El-Sayed, A.R., Mohran, H.S. & Abd El-Lateef, H.M. 2011. Inhibitive action of ferricyanide complex anion on both corrosion and passivation of zinc and zinc–nickel alloy in the alkaline solution. *Journal of Power Sources*, 196(15), pp.6573-6582. Available at: <https://doi.org/10.1016/j.jpowsour.2011.03.057>.

Emel'yanov, A.V., Sapunov, S.Yu. & Kudryakov, O.V. 2009. Principles of controlling crystallization kinetics for a multicomponent coating on steel. *Metallurgist*, 53, pp.648-654. Available at: <https://doi.org/10.1007/s11015-010-9228-y>.

Farina, S.B. & Duffo, G.S. 2007. Corrosion of zinc in simulated carbonated concrete pore solutions. *Electrochimica Acta*, 52(16), pp.5131-5139. Available at: <https://doi.org/10.1016/j.electacta.2007.01.014>.

Hamlaoui, Y., Pedraza, F. & Tifouti, L. 2008. Corrosion monitoring of galvanised coatings through electrochemical impedance spectroscopy. *Corrosion Science*, 50(6), pp.1558-1566. Available at: <https://doi.org/10.1016/j.corsci.2008.02.010>.

Hosseini, M.G., Abdolmaleki, M. & Ashrafpoor, S. 2012. Preparation, characterization, and application of alkaline leached Ni/Zn–Ni binary coatings for electro-oxidation of methanol in alkaline solution. *Journal of Applied*

*Electrochemistry*, 42, pp.153-162. Available at: <https://doi.org/10.1007/s10800-012-0382-8>.

Hsu, C.H. & Mansfeld, F. 2001. Concerning the conversion of the constant phase element parameter  $Y_0$  into a capacitance. *Corrosion*, 57(9), pp.747-748. Available at: <https://doi.org/10.5006/1.3280607>.

Kaesche, H. 1964. The passivity of zinc in aqueous solutions of sodium carbonate and sodium bicarbonate. *Electrochimica Acta*, 9(4), pp.383-394. Available at: [https://doi.org/10.1016/0013-4686\(64\)80044-X](https://doi.org/10.1016/0013-4686(64)80044-X).

Kwon, M., Jo, D., Cho, S., Kim, H., Park, J.T. & Park, J.M. 2016. Characterization of the influence of Ni content on the corrosion resistance of electrodeposited Zn–Ni alloy coatings. *Surface and Coatings Technology*, 288, pp.163-170. Available at: <https://doi.org/10.1016/j.surfcoat.2016.01.027>.

Moreno, M., Morris, W., Alvarez, M. G. & Duffo, G. S. 2004. Corrosion of reinforcing steel in simulated concrete pore solutions. Effect of carbonation and chloride content. *Corrosion Science*, 46(11), pp.2681-2699. Available at: <https://doi.org/10.1016/j.corsci.2004.03.013>.

Mosavat, S.H., Shariat, M.H. & Bahrololoom, M.E. 2012. Study of corrosion performance of electrodeposited nanocrystalline Zn–Ni alloy coatings. *Corrosion Science*, 59, pp.81-87. Available at: <https://doi.org/10.1016/j.corsci.2012.02.012>.

Padilla, V. & Alfantazi, A. 2014. Corrosion film breakdown of galvanized steel in sulphate–chloride solutions. *Construction and Building Materials*, 66, pp.447-457. Available at: <https://doi.org/10.1016/j.conbuildmat.2014.05.053>.

Qiao, X., Guan, H., Zhou, Z., Song, D. 2024. Research Progress in Corrosion Behavior and Anti-Corrosion Methods of Steel Rebar in Concrete. *Metals*, 14(8), art.number:862. Available at: <https://doi.org/10.3390/met14080862>.

Ravindran, V. & Muralidharan, V.S. 2006. Characterization of zinc–nickel alloy electrodeposits obtained from sulphamate bath containing substituted aldehydes. *Bulletin of Materials Science*, 29, pp.293-301. Available at: <https://doi.org/10.1007/BF02706499>.

Roventi, G., Bellezze, T., Barbaresi, E. & Fratesi, R. 2013. Effect of carbonation process on the passivating products of zinc in  $\text{Ca}(\text{OH})_2$  saturated solution. *Materials Corrosion*, 64(11), pp.1007-1014. Available at: <https://doi.org/10.1002/maco.201206868>.

Roventi, G., Bellezze, T., Giuliani, G. & Conti, C. 2014. Corrosion resistance of galvanized steel reinforcements in carbonated concrete: effect of wet–dry cycles in tap water and in chloride solution on the passivating layer. *Cement and Concrete Research*, 65, pp.76-84. Available at: <https://doi.org/10.1016/j.cemconres.2014.07.014>.

Short, N.R., Zhou, S. & Dennis, J.K. 1996. Electrochemical studies on the corrosion of a range of zinc alloy coated steel in alkaline solutions. *Surface and Coatings Technology*, 79(1-3), pp.218-224. Available at: [https://doi.org/10.1016/0257-8972\(95\)02428-X](https://doi.org/10.1016/0257-8972(95)02428-X).

Sistonen, E., Cwirzen, A. & Puttonen, J. 2008. Corrosion mechanism of hot-dip galvanized reinforcement bar in cracked concrete. *Corrosion Science*, 50(12), pp.3416-3428. Available at: <https://doi.org/10.1016/j.corsci.2008.08.050>.



Sriraman, K., Brahimi, S., Szpunar, J., Osborne, J. & Yue, S. 2013. Characterization of corrosion resistance of electrodeposited Zn–Ni Zn and Cd coatings. *Electrochimica Acta*, 105, pp.314-323. Available at: <https://doi.org/10.1016/j.electacta.2013.05.010>.

Tan, Z.Q. & Hansson, C.M. 2008. Effect of surface condition on the initial corrosion of galvanized reinforcing steel embedded in concrete. *Corrosion Science*, 50(9), pp.2512-2522. Available at: <https://doi.org/10.1016/j.corsci.2008.06.035>.

Tian, W., Xie, F.Q., Wu, X.Q. & Yang, Z.Z. 2009. Study on corrosion resistance of electroplating zinc–nickel alloy coatings. *Surface and Interface Analysis*, 41(3), pp.251-254. Available at: <https://doi.org/10.1002/sia.3017>.

Wang, Y.-q., Kong, G., Che, C.-s. 2019. Corrosion Behavior of Zn-Al, Zn-Mg, and Zn-Mg-Al coatings in simulated concrete pore solution. *Corrosion*, 75(2), pp.203-209. Available at: <https://doi.org/10.5006/3029>.

Wilcox, G.D. & Gabe, D.R. 1993. Electrodeposited zinc alloy coatings. *Corrosion Science*, 35(5-8), pp.1251-1258. Available at: [https://doi.org/10.1016/0010-938X\(93\)90345-H](https://doi.org/10.1016/0010-938X(93)90345-H).

Wu, P.-p., Zhang, Z.-z., Xu, F.-j., Deng, K., Nie, K.-b. & Gao, R. 2017. Effect of duty cycle on preparation and corrosion behavior of electrodeposited calcium phosphate coatings on AZ91. *Applied Surface Science*, 426, pp.418-426. Available at: <https://doi.org/10.1016/j.apsusc.2017.07.111>.

Corrosión del acero de refuerzo recubierto de Zn-Ni en soluciones de poros de concreto simuladas

Mihael M. Bučko<sup>a</sup>, **autor de correspondencia**, Ljubica M. Radović<sup>b</sup>, Marko N. Dimitrijević<sup>a</sup>, Radovan M. Karkalić<sup>a</sup>, Jelena B. Bajat<sup>c</sup>

<sup>a</sup> Universidad de Defensa de Belgrado, Academia Militar, Departamento de Ingeniería Química Militar, Belgrado, República de Serbia

<sup>b</sup> Instituto Técnico Militar, Belgrado, República de Serbia

<sup>c</sup> Universidad de Belgrado, Facultad de Tecnología y Metalurgia, Belgrado República de Serbia,

CAMPO: materiales

TIPO DE ARTÍCULO: artículo científico original

**Resumen:**

*Introducción/objetivo: La protección anticorrosión de barras de refuerzo de acero en concreto es una preocupación crítica en ingeniería civil, particularmente para la construcción de estructuras de concreto destinadas a aplicaciones militares. Actualmente, los métodos más importantes para lograr esta protección incluyen la aplicación de recubrimientos sobre barras de refuerzo de acero (como epoxi o zinc galvanizado en caliente), el uso de barras de refuerzo de acero inoxidable, barras de refuerzo compuestas o concreto de alto rendimiento que incorpore inhibidores de corrosión, selladores de superficies, humo de sílice o aditivos de cenizas volantes.*

*Métodos: Este estudio tiene como objetivo determinar si un recubrimiento galvanizado de Zn-Ni de suficiente espesor puede ofrecer una mejor resistencia a la corrosión a largo plazo al acero de refuerzo en concreto en comparación con el recubrimiento tradicional de Zn puro que se usa típicamente para este propósito. Los recubrimientos de Zn-Ni producidos tenían un espesor de 40 µm y contenían aproximadamente un 13% en masa de Ni. La microscopía electrónica de barrido reveló una morfología superficial suave y homogénea, aunque se observaron microfisuras que se extendían por toda la profundidad del recubrimiento. La efectividad protectora de los recubrimientos se evaluó mediante espectroscopía de impedancia electroquímica, con muestras sumergidas en diversos electrolitos que simulan los ambientes químicos presentes en diferentes tipos de concreto.*

*Resultados: Las mediciones indicaron una velocidad de disolución significativamente más lenta del producto de corrosión formado en el recubrimiento de Zn-Ni en ambientes ricos en cloruro, en comparación con el Zn puro.*

*Conclusión: Se puede concluir que la aleación Zn-Ni presenta una alternativa viable al Zn puro para proteger el acero en estructuras de concreto donde se prevé una alta penetración de cloruro.*

*Palabras claves: corrosión de barras de acero, recubrimiento de Zn-Ni, solución de poros de hormigón, galvanoplastia.*

Коррозия арматурной стали, защищенной покрытием из сплава Zn-Ni, в электролитах, имитирующих поры в бетоне

Михаел М. Бучко<sup>а</sup>, **корреспондент**, Любица М. Радович<sup>б</sup>,  
Марко Н. Димитриевич<sup>а</sup>, Радован М. Каркалич<sup>а</sup>, Елена Б. Баят<sup>в</sup>

<sup>а</sup> Университет обороны в г. Белград, Военная академия, департамент  
военного химического инжиниринга, г. Белград, Республика Сербия

<sup>б</sup> Военно-технический институт, г. Белград, Республика Сербия

<sup>в</sup> Белградский университет, факультет технологии и металлургии,  
г. Белград, Республика Сербия

РУБРИКА ГРНТИ: 67.01.97 Коррозия и защита от коррозии

ВИД СТАТЬИ: оригинальная научная статья

**Резюме:**

*Введение/цель: Антикоррозийная защита стальных арматурных стержней в бетоне является важнейшей задачей в гражданском строительстве, особенно при строительстве бетонных конструкций, предназначенных для военного применения. В настоящее время наиболее важными методами обеспечения такой защиты являются нанесение покрытий на стальную арматуру (например, эпоксидных покрытий или покрытий*

методом горячего цинкования), использование арматуры из нержавеющей стали, композитной арматуры или высококачественного бетона, в состав которого входят ингибиторы коррозии, поверхностные герметики, диоксид кремния или летучая зола.

**Методы:** Цель данного исследования – определить, может ли гальваническое покрытие Zn-Ni достаточной толщины обеспечить лучшую и более долгосрочную коррозионную стойкость арматурной стали в бетоне по сравнению с традиционным покрытием из чистого Zn, которое чаще используется в этой цели. Толщина покрытия Zn-Ni составляла 40 мкм и содержала приблизительно 13 мас.%Ni.

**Результаты:** С помощью метода сканирующей электронной микроскопии выявлена гладкая и однородная морфология поверхности, несмотря на микротрещины, проходящие по всей глубине покрытия. Защитная эффективность покрытий оценивалась с помощью электрохимической импедансной спектроскопии. При этом образцы погружались в различные электролиты, имитирующие химическую среду, присутствующую в различных типах бетона.

**Вывод:** На основании результатов исследования можно сделать вывод, что сплав Zn-Ni представляет собой устойчивую альтернативу чистому Zn для защиты стали в бетонных конструкциях с высокой степенью проникновения хлоридов.

**Ключевые слова:** коррозия стальной арматуры, Zn-Ni покрытие, поровый раствор в бетоне, гальванопокрытие.

Корозија арматурног челика заштићеног превлаком легуре Zn-Ni у електролитима који симулирају поре у бетону

Михаел М. Бучко<sup>а</sup>, аутор за преписку, Љубица М. Радовић<sup>б</sup>,  
Марко Н. Димитријевић<sup>а</sup>, Радован М. Каркалић<sup>а</sup>, Јелена Б. Бајат<sup>в</sup>

<sup>а</sup> Универзитет одбране у Београду, Војна академија,  
Катедра војнохемијског инжењерства, Београд, Република Србија

<sup>б</sup> Војнотехнички институт, Београд, Република Србија

<sup>в</sup> Универзитет у Београду, Технолошко-металуршки факултет,  
Београд, Република Србија

ОБЛАСТ: материјали

КАТЕГОРИЈА (ТИП) ЧЛАНКА: оригинални научни рад

Сажетак:

Увод/циљ: Антикоровозна заштита челичне арматуре у бетону представља кључни изазов у грађевинарству, нарочито у изградњи бетонских конструкција намењених за војне сврхе. Тренутно,

најважније методе за постизање ове заштите укључују примену епоксидних или топлоцинкованих превлака, употребу арматуре од нерђајућег челика или композитних материјала, или бетона који садржи инхибиторе корозије, површинске заптиваче, силицијумску прашину или додаток летећег пепела.

**Метод:** Ова студија има за циљ да утврди да ли превлака од легуре Zn-Ni одговарајуће дебљине, нанета електрохемијским таложењем, може дати бољу и дуготрајнију отпорност на корозију арматурног челика у бетону, у поређењу са традиционалном превлаком Zn која се обично примењује у ту сврху. Нанете превлаке Zn-Ni биле су дебљине 40  $\mu\text{m}$  и садржале су око 13 мас. % Ni.

**Резултати:** Снимање електронским микроскопом открило је да су превлаке имале глатку и хомогену морфологију, иако су показивале микропукотине које су се протезале кроз целу њихову дубину. Заштитна ефикасност превлаке оцењена је електрохемијском импеданцијском спектроскопијом, при чему су узорци били потопљени у различите електролите који симулирају хемијске услове присутне у различитим врстама бетона. Мерења су показала знатно мању брзину растварања продукта корозије формираног на превлаци Zn-Ni у електролиту богатом хлоридима, у поређењу са чистим Zn.

**Закључак:** Може се закључити да легура Zn-Ni представља одрживу алтернативу чистом Zn, за заштиту челика у бетонским конструкцијама где се очекује висока пенетрација хлорида.

**Кључне речи:** корозија челичне арматуре, превлака Zn-Ni, електролит у порам бетона, електрохемијско таложење.

EDITORIAL NOTE: The first author of this article, Mihael Bučko, is a current member of the Editorial Board of the *Military Technical Courier*. Therefore, the Editorial Team has ensured that the double blind reviewing process was even more transparent and more rigorous. The Team made additional effort to maintain the integrity of the review and to minimize any bias by having another associate editor handle the review procedure independently of the editor – author in a completely transparent process. The Editorial Team has taken special care that the referee did not recognize the author's identity, thus avoiding the conflict of interest.

Paper received on: 14.02.2024.

Manuscript corrections submitted on: 16.11.2024.

Paper accepted for publishing on: 18.11.2024.

© 2024 The Authors. Published by Vojnotehnički glasnik / Military Technical Courier (www.vtg.mod.gov.rs, vtg.mo.ynp.cpb). This article is an open access article distributed under the terms and conditions of the Creative Commons Attribution license (<http://creativecommons.org/licenses/by/3.0/rs/>).

